sustainability

MDPI

Article

Impact of a Thermal Barrier Coating in Low Heat Rejection Environment Area of a Diesel Engine

Megavath Vijay Kumar [1,*], Thumu Srinivas Reddy [2], Ch. Rami Reddy [3,*], S. Venkata Rami Reddy [4], Mohammad Alsharef [5], Yasser Alharbi [5] and Basem Alamri [5]

[1] Department of Mechanical Engineering, Malla Reddy Engineering College, Secunderabad 500100, India
[2] Department of Electronics and Communication Engineering, Malla Reddy Engineering College, Secunderabad 500100, India
[3] Department of Electrical and Electronics Engineering, Malla Reddy Engineering College, Secunderabad 500100, India
[4] Department of Electrical and Electronics Engineering, JNTUA College of Engineering, Pulivendula 516390, India
[5] Department of Electrical Engineering, College of Engineering, Taif University, P.O. Box 11099, Taif 21944, Saudi Arabia
* Correspondence: vijaykumar.084@mrec.ac.in (M.V.K.); crreddy229@mrec.ac.in (C.R.R.)

Abstract: The most recent developments in Thermal Barrier Coating (TBC) relate to engine performance, manufacturing and other related challenges. TBC on the piston crown and valves to enhance engine characteristics while using diesel and Mahua Methyl Ester (MME) as a petroleum fuel has a great sustainable development. For this utility, a Direct Injection (DI) conventional diesel engine was renewed to an LHR engine by applying 0.5 mm thickness of $3Al_2O_3$-$2SiO_2$ (as TBC) onto the piston crown and valves. The MME is used in the LHR (Low Heat Rejection) engine. For examination, the fuel injector pressure is set at 200 bar. Compared to a standard DI diesel engine, the results demonstrate that the application of TBC boosts brake thermal efficiency to 13.65% at 25% load. The LHR engine's SFC and BTE significantly improved at full load while using MME fuel. The lower temperature of exhaust gases is achieved by combining MME and diesel fuels with TBC. It was observed that both MME with and without TBC significantly reduced the smoke density. In addition, it was exposed that using MME fuel with TBC very slightly reduced carbon monoxide emissions under all loads. It was also shown that MME with TBC significantly reduced environmental hydrocarbon emissions at all loads.

Keywords: mahua methyl ester biodiesel; diesel fuel; thermal barrier coating; low heat rejection engine; environment; renewable energy

Citation: Vijay Kumar, M.; Srinivas Reddy, T.; Rami Reddy, C.; Rami Reddy, S.V.; Alsharef, M.; Alharbi, Y.; Alamri, B. Impact of a Thermal Barrier Coating in Low Heat Rejection Environment Area of a Diesel Engine. *Sustainability* **2022**, *14*, 15801. https://doi.org/10.3390/su142315801

Academic Editor: Jacopo Bacenetti

Received: 13 October 2022
Accepted: 23 November 2022
Published: 28 November 2022

1. Introduction

In India, the production of inedible oil is poor, leading to some development work undertaken by the Government of India for the production of alternative fuel to inedible oils, such as Jatropha, Mahua, Karanja, Linseed, Cotton, Mustard, Neem, etc. In India, most of the states are tribal regions where Mahua seeds are found in abundance [1,2]. The Mahua tree can provide sources from the seventh year of the plantation onward. Mahua seed oil is a common ingredient of Indian hydrogenated fat. The Mahua raw oil is extracted from the seed kernels and its oil appears similarly to semi-solid fat at room temperature, pale yellow due to the high viscosity in oil. Mahua crude oil contains 30 to 40% free acids. During biodiesel production, the manufacturer can produce various products from glycerin [3,4]. Generally, the raw Mahua Oil (MO) has a high percentage of Free Fatty Acids (FFA) and the change in FFA to biodiesel is very much essential in employing the transesterification or esterification process [5,6]. It is also observed that MO's properties and chemical composition are approximately similar to other inedible oil such as Cotton, Neem, Karanja, etc.,

but the Mahua has a high content of viscosity and FFA. Some renowned processes such as transesterification, esterification, dilution, microemulsion and pyrolysis are utilized to reduce the viscosity in order to produce biodiesel. However, transesterification is one of the best processes for obtaining maximum yield with some effective properties compared to diesel properties [7,8]. The impact of n-butanol/diesel blended fuels on the performance and emissions of heavy-duty diesel engines was investigated. The results showed that the engine performed better when 10% n-butanol was combined with diesel [9]. The effect of n-butanol/diesel fuel on engine performance and emission parameters was investigated and the results revealed that n-butanol at 2% and 4% in the blended fuel reduced emission levels [10]. The impact of n-butanol blended fuels on Euro VI diesel engines was investigated. The findings revealed that diesel/n-butanol mixed fuels increased CO and HC emissions while having no influence on NOx emissions [11]. The combustion and exhaust characteristics of an n-butanol/diesel fuel blend were investigated. The results revealed that the 20% n-butanol/diesel blend reduced soot, NOx, and CO emissions by 56.52%, 17.19%, and 30.43%, respectively, when compared to diesel [12]. The combustion and exhaust characteristics of a blended n-butanol/diesel fuel engine were investigated. The results revealed that n-butanol reduced CO and soot emissions while increasing NOx emissions in n-butanol/diesel fuel [13]. Particulate matter emissions from vehicles can be produced directly throughout fuel combustion or through condensation in the air and nucleation during the dilution and cooling of hot tailpipe exhaust [14]. The majority of particles produced by engine combustion are graphitic carbon, with minor amounts of metallic ash, sulfur compounds, and hydrocarbons [15]. Particle number size distributions (PNSDs) and PM emissions from vehicles are influenced by several factors, including engine type such as SI or CI Engines, type of fuel and engine specifications, vehicle operating conditions, particulate filter technology, and atmospheric conditions (temperature, wind speed, and humidity) [16,17]. One of the physical methods for using vegetable oil in a diesel engine that does not require any chemical treatment is microemulsion [18]. Microemulsions are made by combining esters and dispersants (solvents) with or without diesel fuel to form clear, thermodynamically stable oil-surfactant dispersion [19]. As a result of their higher alcohol content, microemulsions have a lower calorific value than diesel; however, these alcohols have a higher latent heat property and can cool the combustion chamber, reducing nozzle coking. The effects of microemulsification and transesterification on the performance of vegetable oil engines using methanol were examined. The effectiveness of methanol/vegetable oil microemulsions is based on employing methanol-based biodiesel as a surfactant. Previous research focused on the impact of co-surfactants and the effect of catalysts in water oil microemulsions produced from various refined and high-free fatty acid (FFA) oils [20,21]. A few thermos-chemical liquefication studies have focused on using waste sludge mixed with various co-surfactants to develop diesel fuel via microemulsion in enhancing its use and the physicochemical properties of the emulsified fuel. However, due to the high carbon waste and low efficiency, more research is required to enhance this technology for large-scale use [22,23]. As per the authors view, during the combustion of IC engines it was noticed that heat loss is one of the major problems and plays a vital role in all aspects of engine operation such as engine efficiency, fuel consumption, and emissions. Due to the loss of heat energy, the engine's performance and efficiency will be reduced. When the combustion gases take place inside the combustion chamber, the heat energy will be rejected to the atmosphere and pass through the other heat transfer modes. The gas temperature and pressure will be lost due to the engine output.

According to the Global Energy Statistical Yearbook 2020, India consumed 1230 TWh of energy in 2019. In comparison to 2018, global consumption increased by 0.7%. Global energy consumption is expected to skyrocket in the coming century. New industrial power generation equipment materials have resulted in more efficient and long-lasting engines to meet increasing energy demands [24]. Turbines generate energy over a long period. Gas turbines are widely used in energy generation and transportation. The material used in turbine engines has a longevity of over 50,000 h when operated at temperatures ranging

from 900 to 1100 °C. The materials will oxidize regardless of how good they are. Protective coatings are commonly used to keep the fabric from further oxidation and corrosion. Surface modification aims to improve or enhance surface properties that aid in corrosion and oxidation resistance. Coatings have become more resistant to deterioration under operational conditions in recent years [25].

Thermal barrier coatings act as heat barriers, preventing heat from spreading throughout the material. TBC plays an important role in safeguarding parts of gas turbines, internal combustion engines, and other high-temperature machines. TBC is a patterned framework that is layered over metallic segments, such as gas turbine blades. TBCs are distinguished by their low heat conductivity; the coating withstands extremely high temperatures when subjected to a heat stream [26,27]. The need for a higher working temperature in today's gas turbines is an ever-increasing process to improve their work productivity. As a result, the extended working temperatures exceed the melting point of nickel-based super alloys, which is deleterious to the chemical and heat-resistant properties of these composites. As a result, it is critical to protect these substrate materials from high operating temperature levels by providing heat protection via TBC's. Many years ago, ceramics were used before the LHR Engines. Cerium is also used in a thermal barrier coating with a high melting point that is spattered on the outside of alloy parts and has a thickness of 120–400 µm. Ceramic materials have a lower heat conduction coefficient and weight than the other materials used in conventional methods [28]. Nowadays, it is observed that ceramic materials have grown to achieve a better performance in diesel engines [29,30]. Lanthanum zirconate (LaZrO) is well-known in aircraft engines for its high melting point and good thermal stability. The thermal properties and failure mechanisms of these advanced TBCs remain difficult to understand [31]. Due to TBC's capacity to shield, which permits greater working temperatures and lowers the cost of cooling systems, this trend will undoubtedly continue, improving component efficiency overall [32]. The significant lengthening of YSZ TBC lifetime with the application of particular transient regimes with medium cooling/heating rates. This would enable the usage of YSZ at surface temperatures much higher than 1200 °C [33,34]. This paper examines the current state of TBCs, including the most recent developments in terms of their performance and manufacture, associated difficulties, and suggestions for their potential usage in severe settings such as diesel engines, aerospace, nuclear, high-temperature, or other.

Consequently, the loss of heat transfer energy in the engine decreases the overall performance. Many experimental studies have been conducted to gain a better understanding of the mechanisms that affect heat transfer within the combustion chamber. Each of these fundamental studies has contributed to understanding heat transfer in the IC engine, with the ultimate goal of improved engine performance and efficiency. Thus, many have demonstrated that the most essential factors affecting heat transfer include engine load, speed, compression ratio, ignition timing, fuel pressure variation, and equivalence ratio. By applying TBC onto the piston crown and valve, the direct injection (DI) conventional diesel engine is transformed into an LHR engine to reduce heat loss [24]. Enhancing the LHR engine with effective TBC promises lower fuel consumption, higher thermal efficiency, lowering emissions and elimination of the cooling system [25]. Several ceramic coatings such as Mullite, AL_2O_3, TiO_2, $CaO/MgO–ZrO_2$ and Yttria-stabilized Zirconia (YSZ), have been used in several engine applications [26,27].The key contributions of this paper are summarized as follows:

- The system was designed to improve the diesel engine with certain modified parameters such as Thermal Barrier Coating on the piston crown and valve surface based on a thorough literature review;
- The conventional diesel engine was aimed renewed to an LHR engine by applying 0.5 mm thickness of $3Al_2O_3$-$2SiO_2$ (as TBC) onto the piston crown and valves;
- In addition, an alternative fuel was used to reduce emissions with a low heat rejection system;

- Mahua oil was selected for investigation with TBC due to more O_2 content present in Mahua oil.

As per the literature survey, further criteria are discussed in choosing the TBC for diesel engines and the Mullite material characteristics are covered in Section 2. The transesterification procedure for creating Mahua Methyl Ester from its raw oil is described in Section 3. The comparison of the various fuel attributes is discussed in Section 4, along with an analysis. The experimental photography and the engine parameters are described in Section 5, alongside their specifications.

2. Low Heat Rejection Engine

Selection of TBC Material for IC Engines

To fulfill the requirement of a suitable TBC, we have to find an appropriate TBC with a good attachment of coating materials that can resist rigorous conditions in the diesel combustion chamber. The essential requirements for an excellent quality TBC are outlined below.

- Chemical inertness;
- Good adherence capability with a metallic substrate;
- Higher melting point of a material;
- Lower thermal conductivity of a material;
- At room temperature, no phase changes take place;
- Same thermal expansion coefficient with the metallic substrate [35,36].

Even though numerous ceramic materials are used as TBC in diesel engines, the physical properties of Mullite, such as thermal conductivity, high corrosion resistance, high hardness, good thermal shock resistance below 1273 K, etc., are promising. There are some physical properties of Mullite as TBC as shown in the below Table 1. From the below table, we can expect that a quality outside layering material is quite suitable for an internal combustion engine's purpose.

Table 1. Properties of Mullite.

Name	Properties				
Mullite ($3Al_2O_3$-$2SiO_2$)	Melting Point	Poisson's Ratio	Thermal Conductivity (λ)	Young's Modulus (E)	Thermal Expansion Coefficient (α)
	2123 K	0.25	3.3 W/mk (1400 K)	127 GPa (293 K)	5.3×10^{-6} (293–1273 K)

The conventional engine was converted into an LHR engine with a Mullite coating in order to improve the engine. For this purpose, one bore diesel engine is transformed into LHR engine by applying the Mullite of 0.5 mm thickness onto the valves and piston crown as shown in Figure 1.Later, experimental work was carried out with standard diesel and biodiesel with and without TBC to analyze the performance and emission characteristics.

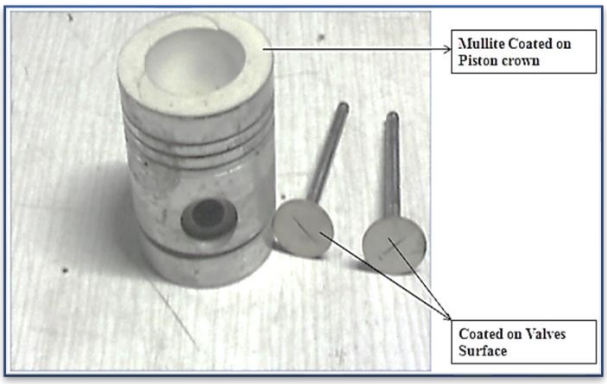

Figure 1. Mullite coated to Piston crown and valves surface.

3. Transesterification Process

In this section, the transesterification process is presented. Initially, the Mahua oil is preheated at 65 °C to 70 °C for 30 min to remove the moisture content. After the preheating process, 1000 mL of Mahua oil is taken with 14 g of potassium hydroxide and 300 mL of methanol. The potassium hydroxide and methanol are added to 1000 mL of Mahua oil, then it is heated at 55 °C and simultaneously the solution has to be stirred for 60 min. During the process, the chemicals react with the Mahua oil and produce the MME. After finishing the process, the mixture is allowed to settle down in a separating flask for 24 h. Once the reaction process is completed, the glycerin must be settled down and the methyl ester should be separated in a separate container. After the separation, the MME should be washed with distilled warm water. The distilled water is heated at 45 °C; then, the heated distilled water is mixed with MME and after mixing the solution, it must be shaken gently to remove residual catalyst or soap content. Then, the distilled water is removed. The MME is then heated at 100 °C for 30 min to remove the trace of water left over in it. Finally, the Mahua biodiesel was obtained as per the methodology of the reference article [37] as shown in Figure 2.

Figure 2. Final Product of Pure Mahua Biodiesel.

4. Fuel Properties

Various physical properties of diesel and MME fuels are mentioned in Table 2. Some of the physical properties, such as density, specific gravity, kinematic viscosity, calorific value, flash point, fire point, Cloud point, pour point and colour, were tested in the fuel laboratory of Malla Reddy Engineering College, India and the rest of the properties were cited [38]. The properties of the MME fuel are within the standard of ASTM D 6751 and EN 14214.

Table 2. Properties of the Fuels.

Properties	Diesel	MME	Test-Method	Instruments Used
Density(15 °C), kg/m^3	835	872	EN ISO 3675/EN ISO 12185	Hydrometer
Specific gravity	0.850	0.916	ASTM D792	Hydrometer
Kinematic viscosity at 40 °C, mm^2/s	2.4	4.0	EN ISO 3104/EN 14105	Redwood Viscometer
Calorific value (KJ/kg)	42,930	39,400	ASTM D240	Bomb Calorimeter
FlashPoint °C	70	127	EN ISO 2719/EN ISO 3679	Pensky-Martens
FirePoint °C	76	136	EN ISO 2719/EN ISO 3679	Pensky-Martens
Cloud point °C	−10 to −15	6	ASTM D2500	Cloud Point
Pour point °C	−35 to −15	1	ASTM D97	Pour Point
Colour	Light brown	Dark yellow	NM	Based on eye visibility
Cetane number	51	46	EN ISO 5165	[38]
Aniline point °C	69	63	EN 14111	[38]
Iodine value	NM	60	ASTM D1959-97	[38]
Diesel index	150	145	NM	[38]

Note: NM = Not measured.

5. Experimental Setup Description

5.1. Engine Test

A 3.5 kW single bore diesel engine (Table 3) with a fixed speed 1500 rpm water cooled is used for the investigation to progress the performance and to diminish the harmful emissions. The layout of the experimentation setup has been depicted in Figure 3. For loading the engine, the eddy current dynamometer has been used for investigation.

Table 3. Engine Specifications.

Name of the Specifications	Values
Name of Engine	Kirloskar
Stroke	4
Type of cooling	Water Cooled
Loading Type	Eddy Current Dynamometer
BHP	5
Stroke length	110 mm
Bore	80 mm
No. of Cylinder	1
Compression Ratio	16.5:1
Speed	1500 rpm
Fuel Injection Pressure	200 bar
Rated output	3.68 kw (5.0 hp)
Connecting Rod Length	230.0 mm
Exhaust Valve Open	20° BBDC [39]
Exhaust Valve Closes	20° ATDC [39]
Inlet Valve Open	20°BTDC [39]
Inlet Valve Close	25° ATDC [39]
Injection Advance	27° BTDC

The fuel has been injected into a cylinder with a pressure of 200 bar. The timing made for valve opening and closing is the exhaust valve opens at 20° BBDC, the exhaust valve closes at 20° ATDC, the inlet valve opens at 20° BTDC and the inlet valve closes at 25° ATDC. The fuel injection timing was maintained at 27° before Top Dead Center. Emission gas analyzers and smoke analyzers were used to find the content of HC, CO, NO_x, and smoke opacity.

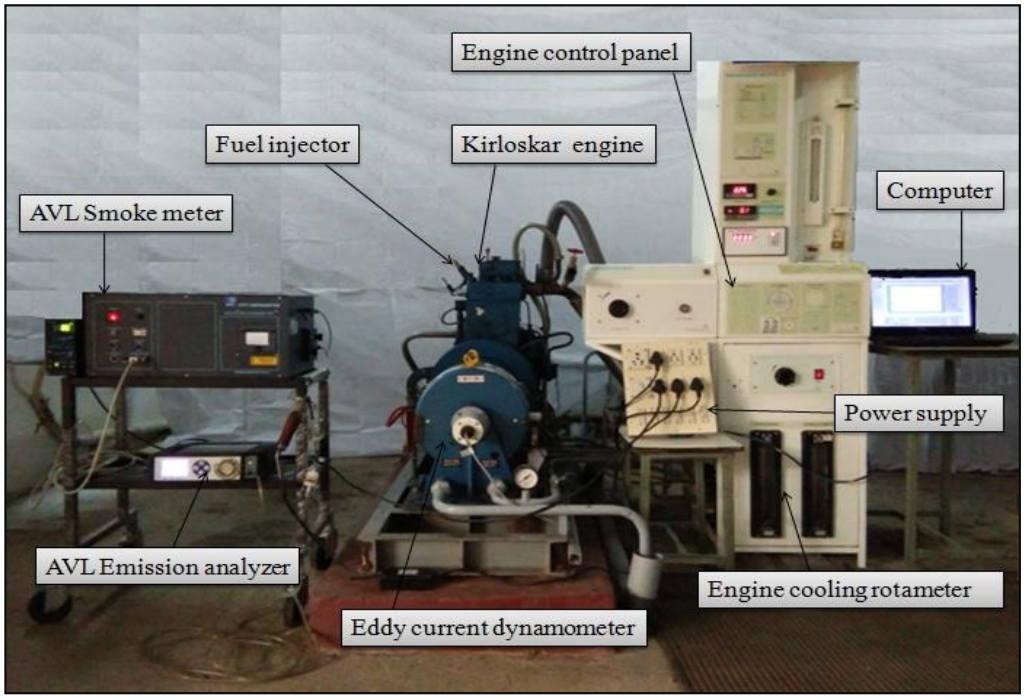

Figure 3. Photograph view of an experimental setup.

5.2. AVL 444 Gas Analyzer

This procedure must be performed on gas analyzers after they have been field-commissioned and for subsequent calibration. The accuracy and measuring ranges are presented in Tables 4 and 5.

Table 4. Gas Analyzer Measuring Range.

S. No.	Measured Parameter	Specification
1	Oxygen	0–22% vol.
2	Carbon monoxide	0–10% vol.
3	Carbon dioxide	0–20% vol.
4	Hydro carbon	0–20,000 ppm
5	Nitrogen oxide	0–5000 ppm
6	Engine speed	400–6000 rpm
7	Oil temperature	30–125 °C
8	Lambda	0 to 9.999

Table 5. Gas Analyser Accuracy.

S. No.	Measured Parameter	Specification
1	Oxygen	<2% vol.: ±0.1% vol. >2% vol.: ±1% vol.
2	Carbon monoxide	<0.6% vol.: ±0.03% vol. >0.6% vol.: ±5% vol.
3	Carbon dioxide	<10% vol.: ±0.5% vol. >10% vol.: ±5% vol.
4	Hydro carbon	<200 ppm: ±10 ppm >200 ppm ±5% of ind. value
5	Nitrogen oxide	<5000 ppm: ±50 ppm
6	Engine speed	±1% of ind. value
7	Oil temperature	±4 °C

The test procedure for gas analyzers is as follows:

- Ensure that the power supply meets the manufacturer's specifications and that the electrical earthing is correct;
- Ensure that all of the accessories specified by the manufacturer are present and functional;
- Validate the span and zero calibration with suitable CO and HC sample gases;
- Examine the electrical calibration;
- Ensure that the sampling system is leak-free;
- The printer is operational, and the printout details are correct;
- Using this analyzer, check one vehicle for idling emission measurement.

5.3. Specification of AVL Smoke Meter and its Operating Conditions

The specifications of AVL smoke meter are presented in Table 6. Operating conditions:

- Warm-up time:20 min (max.) at 220 V Supply;
- Operating temperature:0–50 °C;
- Relative humidity:90% at 50 °C relative humidity (non condensing).

Table 6. Specification of AVL smoke meter.

Type	Values/Model
Make and Model	AVL 437C Smoke meter
Sampling type	Partial flow
Light source	Halogen Lamp, 12 V/5 W
Range	0–100% opacity, 0–99.99 m^{-1} absorption
RPM	400–6000 in

5.4. Percentage Uncertainties of Calculated Parameters

The uncertenities of calculated parameters are shown in Table 7.

Table 7. Uncertainties for Calculated parameters.

Parameters	Percentage Uncertainties
Brake power	±0.5
Brake specific fuel consumption	±1.5
Brake thermal efficiency	±1.0

6. Results and Discussion

At different loadings, the LHR engine was investigated for different diesel and biodiesel with TBC and without TBC. The result was analyzed and is presented in the following sections.

6.1. Performance and Emission Parameters

6.1.1. Brake Specific Fuel Consumption

The variation of brake specific fuel consumption (BSFC) with a load at 200 bar pressure, which shows the results both with and without TBC for different fuels, is presented in Figure 4. Here, the fuel consumption of diesel is lower when compared to biodiesel. The BSFC without TBC of diesel at full load is 0.40 kg/kWh and for biodiesel is 0.44 kg/kWh. The comparison of TBC of diesel at full load is 0.37 kg/kWh and for biodiesel is 0.42 kg/kWh. At 25% load diesel with TBC, fuel consumption was found to be lower. The use of with and without TBC increases biodiesel fuel consumption because of its lower calorific value.

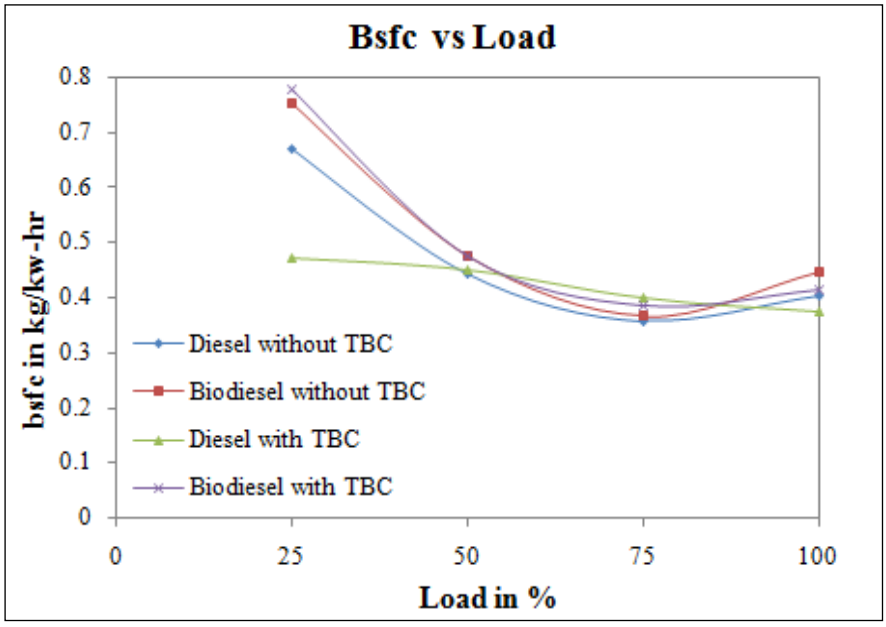

Figure 4. BSFC vs. Load.

6.1.2. Brake Thermal Efficiency

The Figure 5 shows the variation of brake thermal efficiency (BTE) with load at 200 bar pressure. The experiment was conducted with and without TBC for different fuels. At 25% load condition, diesel with TBC was found to be improved. At full load conditions, not much remarkable improvement was observed because higher viscosity leads to poor atomization, fuel vaporization and combustion. Hence, there was not much improvement in thermal efficiency.

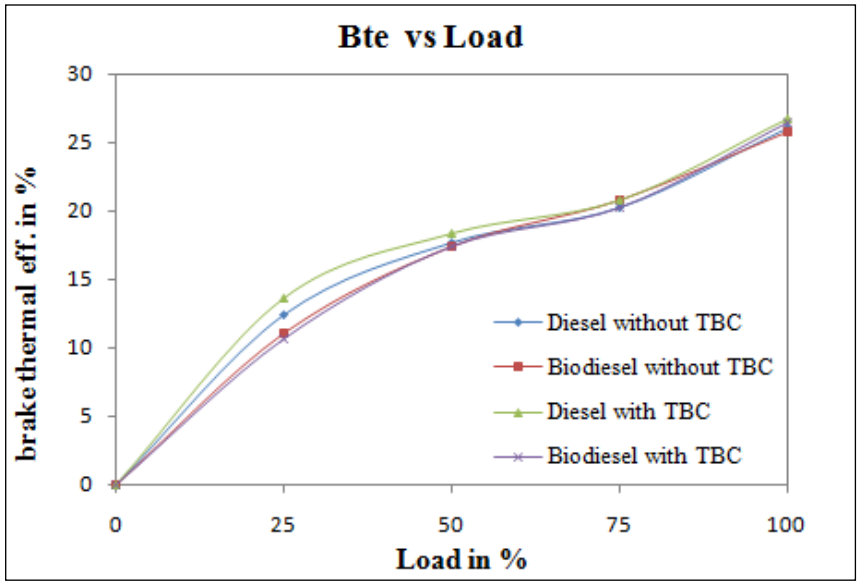

Figure 5. BTE vs. Load.

6.1.3. Exhaust Gas Temperature

Figure 6 shows the variation of exhaust gas temperature with a load at 200 bar injection pressure. The results showed that, in all cases, the exhaust gas temperature increased with the increase in load. For the diesel and biodiesel fueled without TBC, the biodiesel was the highest value of exhaust gas temperature of 265 °C, whereas the corresponding value with diesel was found to be 255 °C; for biodiesel with TBC, the highest value of exhaust gas temperature

was 427 °C, whereas the corresponding value with diesel was found to be 337 °C only. The exhaust temperature having a higher percentage of biodiesel was found to be higher at the entire load in comparison to diesel oil with TBC. The MME and diesel without TBC were found to lower exhaust gas temperature compared to others with TBC. This may be due to the higher combustion temperature of TBC, which gains more heat during the combustion process, and the presence of more oxygen in biodiesel, resulting in a higher peak combustion temperature; this, therefore, increases the exhaust gas temperature for biodiesel at full load.

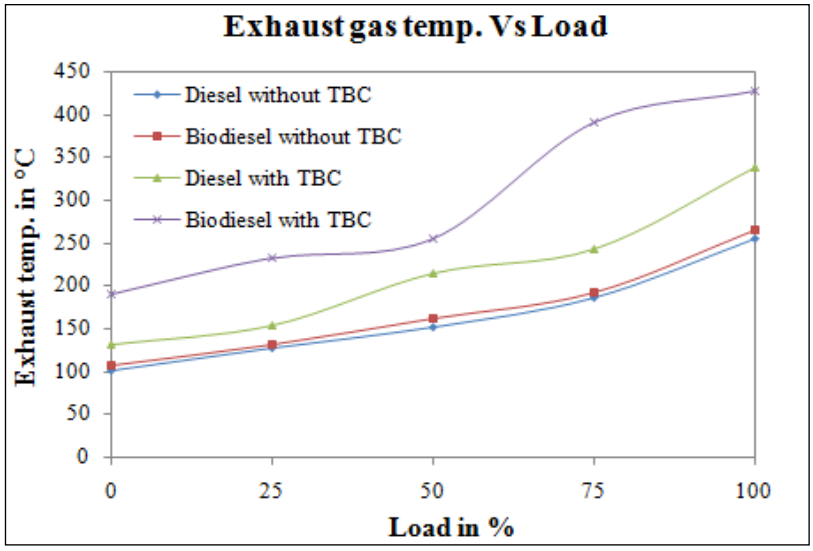

Figure 6. Exhaust Gas Temperature vs. Load.

6.1.4. Smoke Density

The variation of smoke density with load is shown in Figure 7. The smoke density of biodiesel with and without TBC was found significantly reduced compared to diesel with TBC and without TBC. This is because biodiesel has a better vaporization effect at higher combustion temperatures, and there is more oxygen in biodiesel. In comparison to all other trends, the particulate matter has been reduced for biodiesel with TBC because TBC has the ability to resist heat in the combustion chamber, which has aided in the burning of smoke particles.

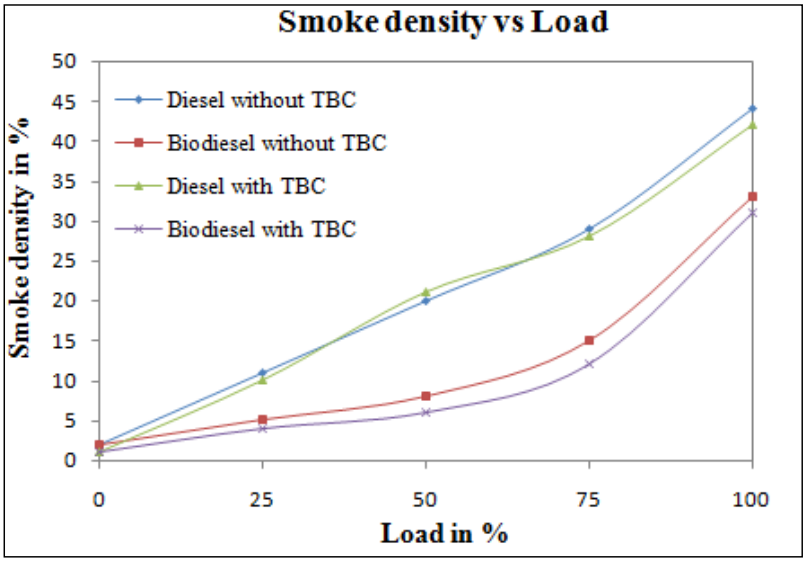

Figure 7. Smoke Density vs. Load.

6.1.5. CO Emissions

Figure 8 shows the variation of carbon monoxide emission with load at 200 bar injection pressure. The results were compared with and without TBC which was fueled with diesel and biodiesel. At 100% load condition, the results were found to increase the CO emissions compared to the different loads such as 0%, 25%, 50% and 75%. At 1% to 75% load, the CO emission was found to be lower because of improvements in combustion and because more oxygen molecules are contained in biodiesel [40]. At all load conditions, the flow rate of the air will be constant, but the fuel flow rate will vary as the load varies. So, as the fuel flow rate increases, the mixture keeps becoming rich. However, in the case of high load, with more amount of fuel and a lower amount of air present, and also as a result of the improper mixing, more carbon monoxide will be released.

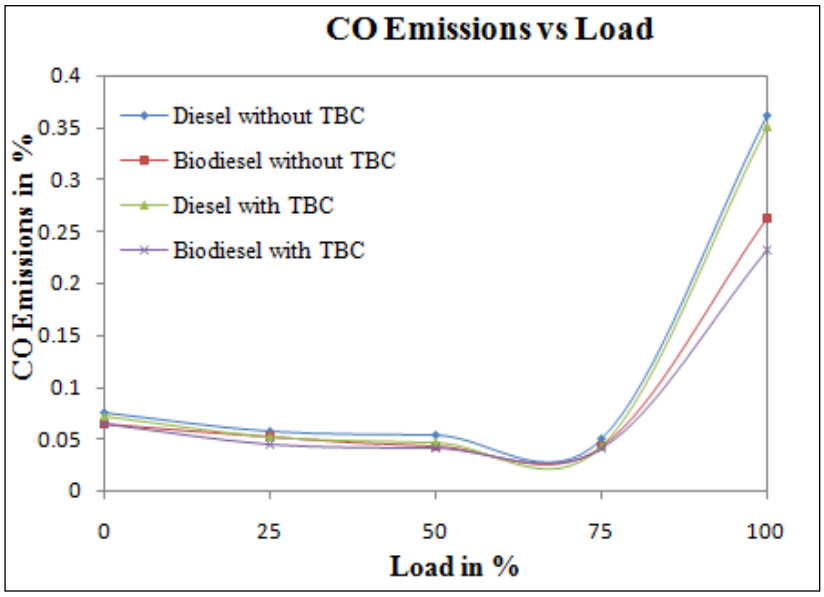

Figure 8. CO Emissions vs. Load.

6.1.6. HC Emissions

The comparisons of hydrocarbon emissions of diesel and biodiesel at 200 bar injection pressure with and without TBC are shown in Figure 9. Biodiesel was found to emit much fewer HC emissions compared to the baseline fuel. At maximum load without TBC, the HC emissions are 90 (PPM) for diesel and for biodiesel 47 (PPM). At 100% load without TBC, biodiesel emits much fewer CO emissions compared to diesel. At maximum load, there was a remarkable reduction in HC emissions: 63 (PPM) for diesel and 45 (PPM) for biodiesel with TBC. The use of thermal barrier coating inside the cylinder resists the high temperature at the surface of the cylinder due to the high temperature, the formation of hydrocarbon will reduce. Additionally, the use of biodiesel with TBC enhances in the reduction in HC due to the oxygen present in biodiesel. This may be owing to an increase in combustion gas temperature as a result of a decline in heat losses.

6.1.7. NOx Emissions

The variation of oxide of nitrogen (NOx) with load at 200 bar pressure, which is shown with and without TBC for diesel and biodiesel fuels, is presented in Figure 10. NOx is formed by oxidizing nitrogen in the atmosphere at a sufficiently high temperature, depending on the number of oxygen ions present. It was well noted that the biodiesel with and without TBC causes more NOx emissions because more O_2 levels are present in biodiesel which helps in better combustion and results in increasing the temperature. The diesel without TBC was found to lower NOx emissions.

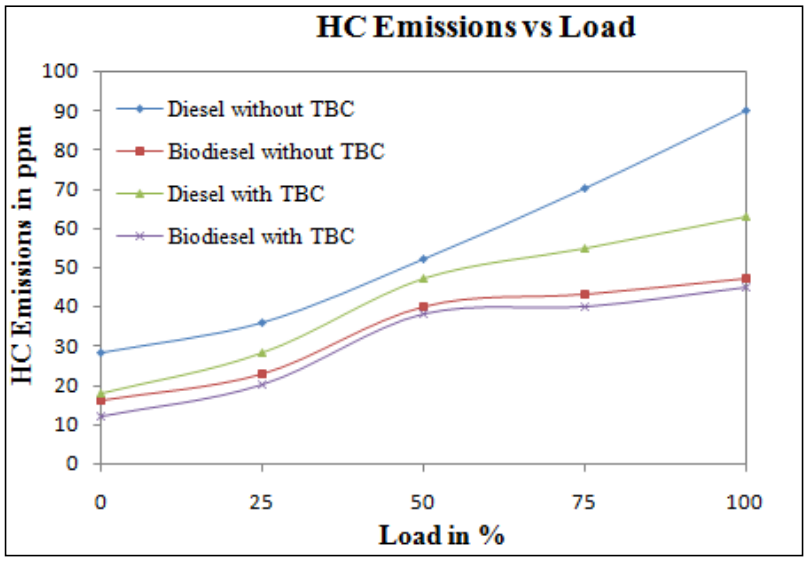

Figure 9. HC Emissions vs. Load.

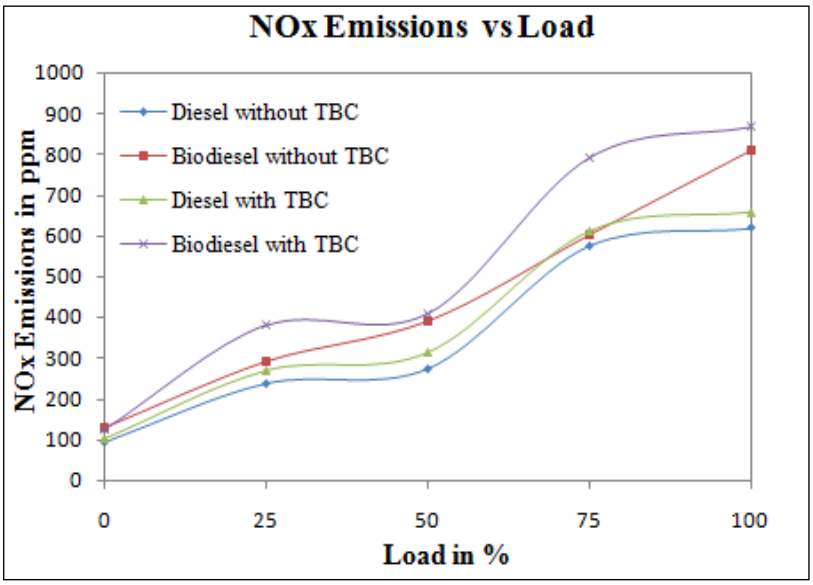

Figure 10. NOx vs. Load.

7. Conclusions

In the current work, to improve engine performance with Mahua biodiesel in CI engines, different technologies with and without TBC have been studied and compared with baseline fuel. Here, experiments were conducted with biodiesel and TBC technologies and have been studied extensively through performance and emissions. The experiments were demonstrated with constant fuel injector pressure of 200 bar and at a constant speed of 1500 rpm. Now that we have conducted the investigation and analysis of the LHR engine, we reveal the important conclusions below.

The Mahua methyl ester properties of density, fire point, flash point, and kinematic viscosity were observed to be within the limits of ASTM D 6751 and EN 14214 specifications. The property value is observed to be sealed and higher than the diesel. The calorific value (CV) of the alternative fuel is seen to be lower than diesel. This will cause an increase in ignition delay during the combustion process in LHR engine.

DI diesel engine was transformed to an LHR engine with the modification of 0.5 mm thickness of $3Al_2O_3$-$2SiO_2$ as TBC onto the piston crown and valves. Later, the engine characteristics were investigated and analyzed.

The fuel consumption of diesel is lower when compared to MME biodiesel. Due to the low calorific value, using and not using the TBC will increase the fuel consumption of biodiesel.

A significant increase in brake thermal efficiency at 25% load condition diesel with TBC was found to be improved due to the TBC.

Using TBC, good results for exhaust gas temperature with diesel and MME were obtained at all loads. The use of thermal barrier coating inside the cylinder resists the high temperature at the surface of the cylinder due to this more heat is attained during combustion by the TBC. A temperature of 427 °C was achieved by biodiesel with TBC high load and 337 °C by diesel with TBC at a high load. The smoke density of MME with and without TBC was found significantly reduced due to the greater amount of O_2 atoms present in the biodiesel and as well as the use of thermal barrier coating inside the cylinder resist the high temperature at the surface.

CO emissions were observed to decrease with the combination of biodiesel and TBC at all loads. This was due to the resistance of heat in a combustion chamber, as well as the biodiesel being given an extra dose of oxygen content in burning. At all loads, MME biodiesel with TBC was found a remarkable reduction in HC emissions. At maximum load, there was a remarkable reduction in HC emissions: 63 (PPM) for diesel and 45 (PPM) for biodiesel with TBC. This happened due to the O_2 molecules present in the MME oil.

It is observed that biodiesel with and without TBC causes more NOx emissions, and that biodiesel with TBC has increased to 870 ppm of NOx emission at high load conditions. High-temperature fuel combustion occurs when a fuel is burned at a temperature high enough (over 1300 °C or 2370 °F) to cause some of the nitrogen in the air to oxidize and produce NOx emissions. The diesel without TBC was found to lower NOx emissions.

As a result, MME biodiesel can be used as a substitute fuel for diesel engines, rather than modified and unmodified diesel fuel. For added benefit, the TBC can be used as a diesel engine substitute fuel.In future works, we can go to further enhance the engine with different alternative fuels and fuel additives. Moreover, to reduce the NOx, it can be investigated with the exhaust gas recirculation system.

Author Contributions: Conceptualization M.V.K., C.R.R.; methodology, S.V.R.R., M.V.K.; software, M.V.K., C.R.R.; validation M.A., Y.A. and B.A.; formal analysis, M.V.K.; investigation, M.V.K. and C.R.R.; resources, M.V.K.; data curation, C.R.R. and T.S.R.; writing—original draft preparation, M.V.K.; writing—review and editing, C.R.R., S.V.R.R., T.S.R., M.A., Y.A. and B.A.; visualization, B.A.; supervision, C.R.R. and T.S.R.; project administration, M.V.K.; funding acquisition, B.A. All authors have read and agreed to the published version of the manuscript.

Funding: The authors would like to acknowledge the financial support received from Taif University Researchers Supporting Project Number (TURSP-2020/278), Taif University, Taif, Saudi Arabia.

Institutional Review Board Statement: Not applicable.

Informed Consent Statement: Not applicable.

Data Availability Statement: Not applicable.

Conflicts of Interest: The authors declare no conflict of interest.

References

1. Nandi, S. Performance of CI engine by using biodiesel-mahua oil. *Am. J. Eng. Res.* **2013**, *2*, 22–47.
2. Padhi, S.K.; Singh, R.K. Optimization of esterification and transesterification of Mahua (Madhuca Indica) oil for production of biodiesel. *J. Chem. Pharm. Res.* **2010**, *2*, 599–608.
3. Agarwal, A.; Das, L.M. Biodiesel Development and Characterization for Use as a Fuel in Compression Ignition Engines. *J. Eng. Gas Turbines Power* **2001**, *123*, 440–447. [CrossRef]
4. Padhi, S.K.; Singh, R.K. Non-edible oils as the potential source for the production of biodiesel in India: A re-view. *J. Chem. Pharm. Res.* **2011**, *3*, 39–49.
5. Vijay Kumar, M.; Veeresh Babu, A.; Ravi Kumar, P. Producing biodiesel from crude Mahua oil by two steps of trans-esterification process. *Aust. J. Mech. Eng.* **2019**, *17*, 2–7. [CrossRef]
6. Azam, M.M.; Waris, A.; Nahar, N. Prospects and potential of fatty acid methyl esters of some non-traditional seed oils for use as biodiesel in India. *Biomass Bioenergy* **2005**, *29*, 293–302. [CrossRef]

7. Chauhan, P.S.; Chhibber, V.K. Non-edible oil as a source of bio-lubricant for industrial applications: A re-view. *Int. J. Eng. Sci. Innov. Technol.* **2013**, *2*, 299–305.
8. Sirurmath, S.; Vikram, P.M.; Das, G. Transesterification of Fish Oil and Performance Study on 4-Stroke CI Engine with Blends of Fish Biodiesel. *IJRET Int. J. Res. Eng. Technol.* **2014**, *3*, 608–612.
9. Tipanluisa, L.; Fonseca, N.; Casanova, J.; López, J.-M. Effect of n-butanol/diesel blends on performance and emissions of a heavy-duty diesel engine tested under the World Harmonised Steady-State cycle. *Fuel* **2021**, *302*, 121204. [CrossRef]
10. Şahin, Z.; Aksu, O.N. Experimental investigation of the effects of using low ratio n-butanol/diesel fuel blends on engine performance and exhaust emissions in a turbocharged DI diesel engine. *Renew. Energy* **2015**, *77*, 279–290. [CrossRef]
11. Lapuerta, M.; Hernández, J.J.; Rodríguez-Fernández, J.; Barba, J.; Ramos, A.; Fernández-Rodríguez, D. Emission benefits from the use of n-butanol blends in a Euro 6 diesel engine. *Int. J. Engine Res.* **2018**, *19*, 1099–1112. [CrossRef]
12. Nayyar, A.; Sharma, D.; Soni, S.L.; Mathur, A. Experimental investigation of performance and emissions of a VCR diesel engine fuelled with n-butanol diesel blends under varying engine parameters. *Environ. Sci. Pollut. Res.* **2017**, *24*, 20315–20329. [CrossRef] [PubMed]
13. Siwale, L.; Kristóf, L.; Adam, T.; Bereczky, A.; Mbarawa, M.; Penninger, A.; Kolesnikov, A. Combustion and emission characteristics of n-butanol/diesel fuel blend in a turbo-charged compres-sion ignition engine. *Fuel* **2013**, *107*, 409–418. [CrossRef]
14. Maricq, M.; Chase, R.; Podsiadlik, D.; Vogt, R. Vehicle exhaust particle size distributions: A comparison of tailpipe and dilution tunnel measure-ments. *SAE Trans.* **1999**, *108*, 721–732.
15. Shi, J.P.; Mark, D.; Harrison, R.M. Characterization of Particles from a Current Technology Heavy-Duty Diesel Engine. *Environ. Sci. Technol.* **2000**, *34*, 748–755. [CrossRef]
16. Myung, C.L.; Park, S. Exhaust nanoparticle emissions from internal combustion engines: A review. *Int. J. Automot. Technol.* **2011**, *13*, 9–22. [CrossRef]
17. Vu, T.V.; Delgado-Saborit, J.M.; Harrison, R.M. Review: Particle number size distributions from seven major sources and implications for source apportionment studies. *Atmos. Environ.* **2015**, *122*, 114–132. [CrossRef]
18. Fangrui, M.; Hanna, M.A. Biodiesel production: A review. *Bioresour. Technol.* **1999**, *70*, 1–15.
19. Yusuf, N.; Kamarudin, S.; Yaakub, Z. Overview on the current trends in biodiesel production. *Energy Convers. Manag.* **2011**, *52*, 2741–2751. [CrossRef]
20. Wellert, S.; Karg, M.; Imhof, H.; Steppin, A.; Altmann, H.J.; Dolle, M.; Richardt, A.; Tiersch, B.; Koetz, J.; Lapp, A.; et al. Structure of biodiesel based bicontinuous microemulsions for environmentally compatible decontamina-tion: A small angle neutron scattering and freeze fracture electron microscopy study. *J. Colloid Interface Sci.* **2008**, *325*, 250–258. [CrossRef]
21. de Jesus, A.; Silva, M.M.; Vale, M.G.R. The use of microemulsion for determination of sodium and potassium in biodiesel by flame atomic absorption spectrometry. *Talanta* **2008**, *74*, 1378–1384. [CrossRef] [PubMed]
22. Ding, X.; Yuan, X.; Leng, L.; Huang, H.; Wang, H.; Shao, J.; Jiang, L.; Chen, X.; Zeng, G. Upgrading Sewage Sludge Liquefaction Bio-Oil by Microemulsification: The Effect of Ethanol as Polar Phase on Solubilization Performance and Fuel Properties. *Energy Fuels* **2017**, *31*, 1574–1582. [CrossRef]
23. Leng, L.; Han, P.; Yuan, X.; Li, J.; Zhou, W. Biodiesel microemulsion upgrading and thermogravimetric study of bio-oil produced by liquefaction of different sludges. *Energy* **2018**, *153*, 1061–1072. [CrossRef]
24. Karaoglanli, A.C.; Dikici, H.; Kucuk, Y. Effects of heat treatment on adhesion strength of thermal barrier coating systems. *Eng. Fail. Anal.* **2013**, *32*, 16–22. [CrossRef]
25. Buyukkaya, E.; Cerit, M. Experimental study of NOx emissions and injection timing of a low heat rejection diesel engine. *Int. J. Therm. Sci.* **2008**, *47*, 1096–1106. [CrossRef]
26. Cao, X.Q.; Vassen, R.; Stoever, D. Ceramic materials for thermal barrier coatings. *J. Eur. Ceram. Soc.* **2004**, *24*, 1–10. [CrossRef]
27. MohamedMusthafa, M.; Sivapirakasam, S.; Udayakumar, M. Comparative studies on fly ash coated low heat rejection diesel engine on performance and emission characteristics fueled by rice bran and pongamia methyl ester and their blend with diesel. *Energy* **2011**, *36*, 2343–2351. [CrossRef]
28. Jia, L.; Wen, T.; Tian, C.; Liu, Z.; Yu, J.; Yuan, L. Preparation and thermophysical properties of RE2CrTaO7 (Y, Sm, Dy, Yb) ceramics for thermal barrier coating applications. *Ceram. Int.* **2022**, *48*, 23814–23820. [CrossRef]
29. Lima, C.; Guilemany, J. Adhesion improvements of Thermal Barrier Coatings with HVOF thermally sprayed bond coats. *Surf. Coatings Technol.* **2007**, *201*, 4694–4701. [CrossRef]
30. Gatowski, J.A. Evaluation of a selectively-cooled single-cylinder 0.5-l Diesel engine. *SAE Trans.* **1990**, *99*, 1580–1591.
31. Shen, Z.; Liu, G.; Dai, J.; He, L.; Mu, R. LaNdZrO thermal barrier coatings by electron beam physical vapor deposition: Morphology, thermal property and failure mechanism. *Chem. Eng. J. Adv.* **2022**, *11*, 100328. [CrossRef]
32. Mondal, K.; Nuñez, L., III; Downey, C.M.; van Rooyen, I.J. Recent advances in the thermal barrier coatings for extreme environments. *Mater. Sci. Energy Technol.* **2021**, *4*, 208–210. [CrossRef]
33. Vaßen, R.; Bakan, E.; Mack, D.E.; Guillon, O. A Perspective on Thermally Sprayed Thermal Barrier Coatings: Current Status and Trends. *J. Therm. Spray Technol.* **2022**, *31*, 685–698. [CrossRef]
34. Mondal, K.; Nuñez, L., III; Downey, C.M.; Van Rooyen, I.J. Thermal barrier coatings overview: Design, manufacturing, and applications in high-temperature industries. *Ind. Eng. Chem. Res.* **2021**, *60*, 6061–6077. [CrossRef]
35. Kamo, R.; Assanis, D.N.; Bryzik, W. Thin Thermal Barrier Coatings for Engines. *SAE Trans.* **1989**, *98*, 131–136. [CrossRef]
36. Abedin, M.J.; Masjuki, H.H.; Kalam, M.A.; Sanjid, A.; Ashraful, A.M. Combustion, performance, and emission characteristics of low heat rejection engine operating on various biodiesels and vegetable oils. *Energy Convers. Manag.* **2014**, *85*, 173–189. [CrossRef]

37. Kumar, M.V.; Veeresh Babu, A.; Ravi Kumar, P. Experimental investigation on mahua methyl ester blended with diesel fuel in a compression ignition diesel engine. *Int. J. Ambient. Energy* **2019**, *40*, 304–316. [CrossRef]
38. Vijay Kumar, M.; Babu, A.V.; Kumar, P.R.; Reddy, S.S. Experimental investigation of the combustion characteristics of Mahua oil biodiesel-diesel blend using a DI diesel engine modified with EGR and nozzle hole orifice diameter. *Biofuel Res. J.* **2018**, *5*, 863–871. [CrossRef]
39. Basaran, H.U.; Ozsoysal, O.A. Effects of application of variable valve timing on the exhaust gas tem-perature improvement in a low-loaded diesel engine. *Appl. Therm. Eng.* **2017**, *122*, 758–767. [CrossRef]
40. Hegab, A.; Dahuwa, K.; Islam, R.; Cairns, A.; Khurana, A.; Shrestha, S.; Francis, R. Plasma electrolytic oxidation thermal barrier coating for reduced heat losses in IC engines. *Appl. Therm. Eng.* **2021**, *196*, 117316. [CrossRef]